J Exp Biol Advance Online Articles. First posted online on 15 August 2013 as doi:10.1242/jeb.089383
Access the most recent version at http://jeb.biologists.org/lookup/doi/10.1242/jeb.089383

Neuromuscular control of hovering wingbeat kinematics in response to distinct flight challenges in the ruby-throated hummingbird (*Archilochus colubris*)

Sajeni Mahalingam[*†] and Kenneth C. Welch Jr.[*‡]

[*]Department of Biological Sciences, University of Toronto Scarborough, Toronto, Ontario, M1C 1A4, Canada

and

Department of Cell & Systems Biology, University of Toronto, Toronto, Ontario, M5S 3G5, Canada

[†]Present address: Department of Biology, McMaster University, Hamilton, Ontario, L8S 4L8, Canada

[‡]Corresponding author; e-mail: kwelch@utsc.utoronto.ca; phone: (416) 208-5100; fax: (416) 287-7676

Keywords: Ruby-throated hummingbirds, *Archilochus colubris*, electromyography, flight muscles, wingbeat kinematics, hovering flight

Running title: Muscle activity in hovering hummingbirds

Summary

While producing one of the highest sustained mass-specific power outputs of any vertebrate, hovering hummingbirds must also precisely modulate the activity of their primary flight muscles to vary wingbeat kinematics and modulate lift production. While recent studies have begun to explore how pectoralis (the primary downstroke muscle) neuromuscular activation and wingbeat kinematics are linked in hummingbirds, it is unclear if different species modulate these features in similar ways, or consistently in response to distinct flight challenges. In addition, little is known about how the antagonist, the supracoracoideus, is modulated to power the symmetrical hovering upstroke. We obtained simultaneous recordings of wingbeat kinematics and electromyograms (EMGs) from the pectoralis and supracoracoideus in ruby-throated hummingbirds (*Archilochus colubris*) while hovering under the following conditions 1) ambient air 2) air density reduction trials 3) submaximal load lifting trials and 4) maximal load lifting trials. Increased power output was achieved through increased stroke amplitude during both treatments, but wingbeat frequency only increased at low air densities. Overall, relative EMG intensity was the best predictor of stroke amplitude and is correlated with angular velocity of the wingtip. The relationship between muscle activation intensity and kinematics was independent of treatment type, indicating reduced drag on the wings in hypodense air did not lead to high wingtip angular velocities independently of increased muscle work. EMG bursts consistently began and ended before muscle shortening under all conditions. During all sustained hovering spike number per burst consistently averaged 1.2 in the pectoralis and 2.0 in the supracoracoideus. The number of spikes increased to 2.5-3 in both muscles during maximal load lifting trials. Despite the relative kinematic symmetry of the hovering downstroke and upstroke, the supracoracoideus was activated ~1 ms earlier, EMG bursts were longer (~0.9 ms), and

exhibited 1.6 times as many spikes per burst. We hypothesize that earlier and more sustained activation of the supracoracoideus fibers is necessary to offset greater compliance resulting from the presence of the supracoracoid tendon.

Introduction

Understanding how flight muscles function has been of particular interest to biologists because these muscles power the most expensive form of locomotion. Several studies have examined how wingbeat kinematics, neuromuscular activation patterns, and mechanical function in the pectoralis, the primary downstroke muscle, vary with forward flight velocity (Tobalske et al., 1997; Hedrick et al., 2003; Ellerby and Askew, 2007; Tobalske et al., 2010). In agreement with recent work quantifying metabolic power input as a function of flight velocity (Tobalske et al., 2003; Askew and Ellerby, 2007) these studies have generally noted a U-shaped power curve and a similar pattern in the electromyographic (EMG) recordings, with power output and EMG intensity greatest at either velocity extreme and lowest at moderate speeds. Fewer studies have examined variation in power output or EMG activity in the primary upstroke muscle, the supracoracoideus (e.g. Tobalske et al., 1997; Tobalske and Biewener, 2008; Tobalske et al., 2010). Some studies show that variation in neuromuscular activation in the supracoracoideus as a function of flight velocity is similar to that seen in the pectoralis (Tobalske et al., 1997; Tobalske et al. 2010). However, the difference in aerodynamic activity of the upstroke and downstroke during forward flight, as well as the fact that some birds can, with training, achieve takeoff flight without the use of the surpacoracoideus (Degernes and Feduccia, 2001; Sokoloff et al., 2001), suggest that the role of the supracoracoideus in powering some flight styles is not easily predicted.

The unique flight of hummingbirds is facilitated by an upstroke that contributes much more to overall lift production than occurs in other birds during hovering. In hovering hummingbirds, lift generation during the upstroke is partly the result of a) a stroke plane which is roughly horizontal and b) rotation of the wing along its long axis (Warrick et al., 2005, 2009). The features contribute to a hovering wingbeat with greater kinematic symmetry than is observed in other birds (Warrick et al., 2005, 2009). This kinematic symmetry implies greater similarity in mechanical power output from the muscles which power the downstroke and upstroke, the pectoralis and supracoracoideus, respectively. In addition, the supracoracoideus is relatively larger in hummingbirds, at approximately half the size of the pectoralis (Greenwalt, 1962; Tobalske et al., 2010). Greater wingbeat symmetry (Warrick et al., 2005, 2009) and greater morphological similarity (Greenwalt, 1962; Tobalske et al., 2010) suggest potentially greater correspondence in mechanical function and neuromuscular activation patterning between these muscles than is seen in other birds.

Laboratory investigations into the modulation of power output and wingbeat kinematics during hovering flight have traditionally imposed one of two challenges: flight in hypodense air mixtures (e.g. Chai and Dudley, 1995; 1996; Altshuler et al., 2010), or the lifting of additional mass (Wells, 1993). Studies have revealed variation in the kinematic strategies hummingbirds can adopt to increase power output related to differences in the nature of the challenge or possibly to differences among species. During flight in hypodense air in laboratory settings, investigators have reported that ruby-throated (*Archilochus colubris*; Chai and Dudley, 1995; 1996) and Anna's hummingbirds (*Calypte anna*; Altshuler et al., 2010) increase stroke amplitude and wingbeat frequency as air density decreased. Researchers have also reported that stroke amplitude during hovering is greater at higher elevation for species found along natural

elevational gradients in the field (Altshuler et al., 2004; Altshuler and Dudley, 2003). In contrast, Wells (1993) found that broad-tailed (*Selasphorus platycercus*) and rufous hummingbirds (*S. rufus*) that lifted sub-maximal loads increased stroke amplitude but that wingbeat frequency remained constant.

Recently, there has been a resurgence of interest in the neuromuscular control of variation in power output and wingbeat kinematics during flight in hummingbirds (e.g. Altshuler et al., 2010; 2012; Tobalske et al., 2010). Beginning in 1968 with a study by Hagiwara et al. and continuing more recently, investigators have reported unique EMGs from the major flight muscles consisting of one to a few discrete spikes with each wingbeat (Hagiwara et al., 1968; Altshuler et al., 2010; Tobalske, 2010). The simple nature of the EMG waveforms in the hummingbird pectoralis has permitted unique insights into how neuromuscular control, motor unit recruitment, and kinematic performance are related. Altshuler et al. (2010) have shown that Anna's hummingbirds achieve increased stroke amplitude in hypodense air via progressive spatial recruitment of pectoralis motor units, but that temporal recruitment is also required when both stroke amplitude and wingbeat frequency are dramatically increased during brief asymptotic maximal load lifting. Tobalske et al. (2010), reported that rufous hummingbird pectoralis and supracoracoideus EMGs varied in similar ways as birds flew at a range of forward flight velocities. Nonetheless, we do not understand how variation in the neuromuscular control of the supracoracoideus during hovering flight (e.g. timing of activation, number of spikes per burst, or intensity) compares to that of the pectoralis. Additionally, it remains unclear whether differences in observed variation in wingbeat kinematics among species challenged either by submaximal load lifting or flight in hypodense air are the result of variation in motor recruitment patterns, or

are the result of differences in the amount of drag the wing encounters during flight in fluids of differing density.

To address these questions we studied individual ruby-throated hummingbirds as we challenged flight performance in four distinct ways (see figure 1): hovering in normodense air, hovering in progressively less dense air mixtures, the sustainable lifting of progressively greater submaximal loads in normodense air, and the brief lifting of maximal loads in normodense air. During each challenge we obtained high speed video recordings in order to determine wingbeat frequency, stroke amplitude, and the mean angular velocity of the wing tip. In addition, we simultaneously recorded EMG waveforms from both the pectoralis and supracoracoideus muscles in order to determine the number of spikes, rectified EMG area (intensity), and timing of EMG bursts relative to wingbeat transitions (i.e. pronation or supination events, respectively).

Methods

Experimental Animals

Four adult male ruby-throated hummingbirds (*Archilochus colubris*) were captured in Scarborough, ON, Canada. The birds were housed individually in 61 by 61 by 61 cm cages. Birds were fed Nektar Plus (Nekton, Kieselbronnerstr. 28, Pforzheim, Germany) *ad libitum* and were maintained on a 14:10 L/D cycle. Individual mass averaged 2.81 ± 0.09 g during the experiments, determined by averaging each individual's mass measured at the beginning and at the end of the experiment. Capture of animals was accomplished under permit from the Canadian Wildlife Service in Ontario. All procedures were approved by the University of Toronto Laboratory Animal Care Committee.

Surgical Procedures

Muscle activation patterning was recorded from both the pectoralis and supracoracoideus. Implantation of electrodes and approaches used in the collection of electromyographic activity followed protocols described in Altshuler et al. (2010). To accomplish electrode implantation birds were anaesthetized using vaporized isoflurane and maintained on a heating pad. The skin above the pectoralis was cleaned with Betadine Solution (Purdue Pharma, Pickering, Ontario, Canada) and feathers were brushed aside or removed, when necessary. Two bipolar electrodes were each made from a pair of 0.08 mm diameter bifilar HML-insulated silver wires (California Fine Wine Wire Company, Grover Beach, California, USA). The tips of each lead in each bipolar electrode were offset by approximately 0.5mm and stripped of insulation at the first 0.5mm of each lead. The terminal ~1 mm of each electrode was inserted into a 26 gauge needle and bent 180 degrees in order to form a hook. One of the bipolar electrodes was inserted into the left pectoralis muscle (Figure 2A). Once inserted, the electrode was held in place using fine forceps, while the needle was removed. The hook at the end of the electrode kept the wire embedded in the muscle. The electrode lead was sutured (6-0, silk suture) to the skin above the pectoralis. The same procedure was followed for the implantation of the electrode into the left supracoracoideus muscle; however, the needle was inserted more deeply and at a location medial to the insertion of the first electrode (Figure 2B). A third, monofilar, insulated silver wire (HML, California Fine Wine Wire Company) was stripped of insulation for the first 0.5mm of the lead and was similarly implanted under the skin on the bird's dorsal surface above the vertebral column and served as a ground electrode. The bipolar electrodes inserted into the pectoralis and supracoracoideus were fed cranially and dorsally over the left shoulder joint and then caudally along the back, running near the point of insertion of the ground electrode. All three wires were

then sutured together on the intervertebral fascia on the dorsal side of the animal. Figure 2 illustrates the approximate location of placement of each of the two bipolar recording electrodes. Once the surgery was complete the anaesthesia was removed and the birds were allowed to recover. Recovery was considered complete when birds were readily able to sustain hover-feeding.

Experimental Design

The experiment was conducted in a testing arena that was 61cm in width by 62cm in length by 76cm in height. Beginning several days prior to data collection the birds were trained to perch, fly and feed, both unweighted and while wearing small weights (see below). A 1ml disposable syringe served as the artificial feeder. Birds were trained to hover feed on command by occluding the feeder opening with a small shield and allowing access for only brief durations at regular intervals every 10-20 minutes. Muscle activation and wingbeat kinematics were studied for all four birds under the following conditions: (1) hovering at a feeder (in ambient air without any load attached) (Chai and Dudley, 1996; Chai et al., 1997; Altshuler et al., 2010), (2) hovering at a feeder in progressively less dense normoxic (heliox-ambient) air mixtures (Chai and Dudley, 1996; Altshuler et al., 2010), (3) hovering at a feeder while lifting progressively heavier sub-maximal loads (Wells, 1993), and (4) hovering briefly while lifting maximal loads (Figure 1) (Chai et al., 1997; Altshuler et al., 2004; Altshuler et al., 2010).

Air density was reduced in the air tight test arena by progressive replacement of normal air at Scarborough, Ontario, Canada (elevation= 76m, density = 1.178 kg m^{-3}) with normoxic heliox (21% oxygen, balance helium; density=0.41 kg m^{-3}) at a rate of 8.5 l min^{-1}. Air density was calculated following measurement of barometric pressure, temperature and humidity.

Following each hover feeding event, a Galton whistle was blown inside the arena and fundamental changes in frequency were used to calculate the reduced air density, relative to normal (as in Altshuler et al., 2010). Through trial and error we were able to time hover feeding events to coincide with air density values of approximately 1, 0.9, 0.8 and 0.7 kg m^{-3}. Birds consistently failed to sustain hovering at the artificial feeder at densities lower than 0.7 kg m^{-3}.

Following density reduction feeding trials, the door to the chamber was opened and density inside the chamber was allowed to return to normal. Then, after recording data during at least one subsequent feeding while hovering in normal air, birds were subjected to a series of load lifting trials. Submaximal loads consisting of a short string of beads connected to a rubber harness were applied to birds by placing the harness around an individual's neck. Loads with total masses of 0.25, 0.5 or 0.75 grams were constructed prior to data collection. Birds were accustomed to perching and hover-feeding while wearing loads during training periods prior to data collection (see above). Recordings were collected of birds hover-feeding while lifting each submaximal load in a randomized order. Recordings were discarded from analysis when any individual was not able to fly from the perch, feed for a minimum of 2 seconds, and fly back to the perch successfully, as failure to do so was taken as indication that the bird could not sustain the load.

Following all submaximal load lifting trials, the harness was removed and the bird was allowed to recover for a minimum of 20 minutes. Then, data were recorded while the unloaded bird hover-fed in normodense air. Following this baseline trial, birds were subjected to maximum load lifting trials. The attachment of weight via a harness placed around the neck was identical to that employed during submaximal load lifting except that the chain was significantly longer and included beads of known individual mass and spaced at ~1 cm intervals, weighing collectively

more than the hummingbird could lift. Birds were released from the floor of the arena and promptly flew directly upwards, as is their natural escape response, lifting progressively greater weight, until reaching a maximum elevation and load. Birds transiently hovered while lifting this maximal load before descending. A minimum of 3 maximal load lifting trials were recorded, until we were satisfied maximum flight effort had been elicited. A camera captured video from a side view which allowed us to determine the number of beads, and thus maximum mass, lifted. The trial that resulted in the bird lifting the maximum number of beads was chosen for further analysis. A recording of unweighted hover feeding in normodense air was obtained following the maximal load lifting trial. The electrodes were then removed from the bird under anaesthesia.

Electromyography

During each trial listed above, the electrode wires coming from the bird remained connected to cable leads near the bottom edge of the arena. Sufficient electrode lengths were employed such that the leads remained slack at all times, and the lifted length never exceeded ~70 cm. EMG signals were amplified 1000 × with an extracellular amplifier (A-M Systems, Differential AC Amplifier, model 1700, Sequim, WA, USA). Amplifier filters were set to low and high frequency cut-offs of 0.1 Hz and 10 KHz, respectively. The analog signals were acquired using an analog-to-digital converter (Digidata 1440A, Molecular Devices, California, USA) sampling at 10KHz. EMG signals were recorded to PC using Axoscope (v.10.3, Molecular Devices) and were synchronized with high speed video recordings via 2 mechanisms (see below). The TTL signal which triggered the end of video recording was acquired on an additional channel of the amplifier. An additional analog to digital converter was also used, and both electromyographic (including the trigger) and videographic data were simultaneously

recorded to PC using MIDAS DA (Xcitex, Massachusetts, USA). This National Instruments (Austin, Texas, US) analog-to-digital converter was not as precise because it recorded at maximum frequency of 1000 Hz. However, it provided an independent means of confirming synchronization of the EMGs and video data. To facilitate statistical analysis and comparisons among individuals and among muscles, the EMG signals were post-processed. A zero-phase, forth-order high-pass Butterworth filter with a cut-off frequency set at approximately 12 times the wingbeat frequency was used to remove movement artifacts and set the mean of the inactive portions of the signal to zero. EMG area (the rectified area of each EMG burst), EMG amplitude (height of each spike within each burst), EMG onset (start of EMG activity prior to the beginning of the downstroke for the pectoralis and the start of EMG activity prior to the beginning of the upstroke for the supracoracoideus) and number of spikes per burst were calculated as in Altshuler et al., 2010. The spike threshold was set to 0.25 times the highest spike amplitude during each run, in order to automate the detection of discrete spikes and determine the number of spikes per burst. EMG spike amplitude and EMG area were each normalized against the maximum EMG spike amplitude or area, respectively, for each bird across all trials.

Kinematic Analysis

All flight trials were filmed using a high speed video camera (S-PRI, AOS technologies AG, Baden Daettwil, Switzerland) which recorded at 1000 frames per second at shutter speed of 250 µs. The camera was located above the arena and recorded video from an overhead view. Wingbeat frequency was calculated by dividing the recording frequency by the number of frames necessary for completion of a full wingbeat. Stroke amplitude was calculated by deriving the angular distance covered by each wing from the top of the upstroke (wrist pronation) to the

bottom of the downstroke (wrist supination) rotating about each shoulder. At each of these extreme positions, the wings appeared as thin lines when viewed from above. The same 15 consecutive wingbeats were analyzed for both wingbeat kinematics and EMG characteristics. Only wingbeats which occurred when the bird was stationary at the feeder, or relatively stationary and at a maximum elevation during asymptotic load lifting trials, were analyzed. Angular velocity was calculated by dividing stroke amplitude (in radians) by the time taken to complete a half stroke.

Morphological Measurements

The mass of each bird was measured at the beginning and end of each experiment using a digital balance with a precision of 0.1 mg (MS-104S, Mettler Toledo, Switzerland). The mean of the two measurements constituted the estimated mass of the bird during all trials.

Statistical Analysis

All kinematic and EMG variables were averaged across the 15 analyzed wingbeats for each bird within each treatment. Data were analyzed using repeated measures ANOVA using the statistical program, SPSS (v.17.0, IBM, United States) to test for statistically significant differences among treatment means in EMG and kinematic parameters as a function of treatment level. Muscle type was included as a factor to test for differences in EMG parameters between the supracoracoideus and pectoralis. Because birds were similar in mass, and because the maximum loads each bird lifted were also quite similar (1.92 ± 0.14), mass lifted values were binned at average values of 2.8, 3.05, 3.3, 3.55 and 4.72 (for max load lifting). If the data violated the test of sphericity, the Greenhouse-Geisser, Huynh-Feldt, and Lower Bound

correction factors were applied to adjust the degree of freedoms and significance values. Lower bound corrected values are reported because the lower bound correction is the most conservative of the three. A mixed effects non-linear model incorporating individual as a random factor was fitted using the lme4 package (v. 0.999999-2) in the statistical program R (v. 2.15.3) in order to examine whether experiment type, load lifting versus air density reduction, was a significant factor influencing the relationship between neuromuscular activation intensity (EMG area) and angular velocity of the wing tip. Results were considered significant if P-values were less than 0.05. Data are presented below as the mean ± SD of values of the four birds.

Results

Regulation of wingbeat kinematics via neural input across varying aerodynamic power output requirements

Wingbeat kinematics as a function of either total mass lifted or air density are shown in Figure 3. Within air density reduction trials, stroke amplitude increased significantly from 140.9 ± 11.2 degrees in ambient air to 160.9 ± 6.8 degrees in the lowest air density ($F_{4,12} = 17.47$, $P < 0.03$; Figure 3A); however, stroke amplitude never reached values as high as those observed during maximal load lifting assays, see below. Wingbeat frequency increased significantly as a function of declining air density ($F_{4,12} = 4.55$, $P = 0.02$; Figure 3B). However, this trend was driven by the value at the lowest air density (58 ± 3 Hz at 0.7 kg m^{-3}) and wingbeat frequency did not vary significantly as a function of air density when the lowest air density trials were excluded (54 ± 2 to 56 ± 2 Hz between 1.2 and 0.8 kg m^{-3}; $F_{3,9} = 1.29$, $P = 0.34$). Stroke amplitude increased significantly as the birds hover fed while lifting progressively heavier loads ranging from 140.9 ± 11.2 degrees when birds were unloaded (2.8 g total) to 157.3 ± 10.8

degrees while lifting a total of 3.55 g ($F_{1,3}$ = 24.35, P = 0.02; Figure 3C). During maximal load lifting trials (68.22 ± 5.43% of body mass was briefly lifted) stroke amplitudes reached an average of 174.3 ± 5.1 degrees, which is close to the geometrical constraint of approximately 180 degrees (Figure 3C). Wingbeat frequency did not vary significantly among sub-maximal load lifting trials, ranging from 54 ± 3 to 57 ± 2 Hz ($F_{3,9}$ = 1.29, P = 0.34; Figure 3D). Wingbeat frequency was 57 ± 2 Hz during maximal load lifting, which was not significantly greater than the wingbeat frequencies exhibited during sub-maximal load lifting ($F_{4,12}$ = 1.26, P = 0.34: Figure 3D).

As a first step in analysing EMG data, the hovering trials that were conducted in normodense air at the beginning of the experiment and between the different flight challenges were compared. We found no significant differences in wingbeat kinematics or electromyographic waveforms (see below) from either the pectoralis or supracoracoideus across each of the unweighted hover feedings in normodense air (data not shown). This confirmed electrode placement did not change throughout the trial period.

Sample EMG traces from the pectoralis and supracoracoideus shown in Figure 4 are direct outputs from the amplifier with analog filter cut-offs of 1Hz and 10 kHz, prior to any post processing. EMG traces from the pectoralis and the supracoracoideus muscles of ruby-throated hummingbirds are composed of a discrete number of spikes per burst during hovering flight under both load lifting trials and air density reduction trials. Whenever the hummingbirds sustained hovering at the feeder; regardless of the flight challenge, the number of spikes per burst averaged 1-2 spikes per burst (see Figure 5A and 5C). However, this increased to 2.5-3 spikes per burst during maximal load lifting assays. Across air density reduction trials the number of spikes did not increase significantly; the pectoralis exhibited an average of 1.35 ± 0.23 spikes per

burst ($F_{4,12}$ = 2.82, P = 0.07); whereas, the supracoracoideus exhibited 1.90 ± 0.36 spikes per burst ($F_{4,12}$ = 27.874, P = 0.67; Figure 5A). Across all sub-maximal load lifting trials the number of spikes per burst did not increase significantly; the pectoralis exhibited an average of 1.32 ± 0.28 spikes per burst ($F_{1,3}$= 1.27, P = 0.34) and the supracoracoideus exhibited 1.78 ± 0.32 spikes per burst ($F_{1,3}$ = 2.43, P = 0.22; Figure 5C). Compared to the mean values across submaximal load lifting trials, the number of spikes per burst increased significantly during maximal asymptotic load lifting trials; the pectoralis exhibited 2.57 ± 0.38 spikes per burst ($F_{4,12}$ = 22.39, P < 0.001) and the supracoracoideus exhibited 2.8 ± 0.59 spikes per burst on average ($F_{4,12}$ = 5.78, P = 0.008).

Normalized EMG area (EMG area) increased significantly for the pectoralis from 0.30 ± 0.04 to 0.58 ± 0.02 (F4,12 =5.92, P = 0.007) and for the supracoracoideus muscle from 0.31 ± 0.11 to 0.51 ± 0.10 (F4,12 = 5.81, P = 0.008) under air density reduction trials (Figure 5B). EMG area of both flight muscles increased significantly across submaximal load lifting assays and further during maximum load lifting (Figure 5D). EMG area in the pectoralis increased significantly from 0.30 ± 0.04 to 0.86 ± 0.07 (F1,3 = 46.17, P = 0.007) as birds lifted 2.81 ± 0.09 g to the maximum load. EMG area also increased for the supracoracoideus from 0.31 ± 0.11 to 0.85 ± 0.05 as more mass was lifted (F1,3 = 75.50, P = 0.003). Some studies have used normalized EMG amplitude instead of normalized EMG area as a measure of the number of active motor units, but analysis of normalized EMG amplitude of the largest peak within a burst did not vary significantly when birds were lifting heavier loads or hovering in reduced air densities.

The activation of antagonistic muscles were completely out of phase with one another, with very little variation in timing relative to the wing stroke transition. Both the pectoralis and

supracoracoideus muscles were activated and deactivated prior to the start of muscle shortening (as indicated by wing movement). The timing of activation of the of the pectoralis muscle did not vary significantly across air density reduction trials, occurring on average 4 ms prior to the start of the downstroke ($F_{4,12} = 0.31$, $P = 0.87$; Figure 6A). The timing of activation of the supracoracoideus muscle was also constant, occurring on average 5 ms prior to the start of the upstroke ($F_{4,12} = 0.69$, $P = 0.61$; Figure 6A). Though the number of spikes per burst did not vary, EMG duration (measured from the start of first spike to the end of the final spike in the burst) increased significantly as air density decreased in both the pectoralis ($F_{4,12} = 15.23$, $P < 0.0001$) and the supracoracoideus ($F_{4,12} = 29.42$, $P < 0.0001$; Figure 6B). The pectoralis EMG durations ranged from 1.45 ms to a maximum of 2.97 ms across air densities (7.48% to 18.27% of the wingbeat). The supracoracoideus EMG durations ranged from 1.72 to 4.22 ms (8.79% to 25.71% of the wingbeat). The timing of activation of the pectoralis muscle prior to the downstroke did not vary significantly among load lifting trials, occurring 4 ms prior to the start of the downstroke ($F_{4,12} = 1.00$, $P = 0.45$; Figure 6C) . Similarly the onset of EMGs of the supracoracoideus prior to the upstroke did not vary among load lifting trials, occurring 5 ms prior to the start of the upstroke ($F_{4,12} = 2.05$, $P = 0.15$; Figure 6C). EMG duration also increased significantly as the birds lifted greater loads for both the pectoralis ($F_{4,12} = 28.67$, $P < 0.0001$) and the supracoracoideus ($F_{4,12} = 29.42$, $P < 0.0001$; Figure 6D). Under load lifting trials the EMG durations of the pectoralis and supracoracoideus ranged from 1.49 to 4.61 ms (7.64% to 24.76% of the wingbeat) and 1.72 to 5.35 ms (8.79% to 28.55% of the wingbeat); respectively.

Comparing the activation patterns of the supracoracoideus and the pectoralis

The difference between the mean values of all four EMG parameters of the pectoralis and supracoracoideus followed the same patterns within both air density reduction and load lifting trials. On average, normalized EMG area did not significantly differ between the two muscles across air density reduction trials (Figure 5B) ($F_{1,6} = 0.770$, $P = 0.414$) or among load lifting trials (Figure 5D) ($F1,6 = 0.025$, $P = 0.88$). Hence, the intensity of activation of motor units, relative to the maximal activation observed at any point during the trials, did not differ between the two primary flight muscles.

The number of spikes per burst was significantly greater in the supracoracoideus than the pectoralis within both air density trials and load lifting trials. Across all the air density reduction trials the supracoracoideus exhibited 0.77 ± 0.26 more spikes per burst (1.61 times as many spikes per burst) than the pectoralis (Figure 5A) ($F_{1,6} = 27.874$, $P = 0.002$). Across all sub-maximal load lifting trials the supracoracoideus exhibited 0.68 ± 0.27 more spikes per burst (1.55 times as many spikes per burst) than the pectoralis (Figure 5C) ($F_{1,6} = 20.52$, $P = 0.004$). During maximal load lifting the supracoracoideus exhibited 0.23 ± 0.60 more spikes per burst (1.08 times as many spikes per burst) than the pectoralis ($F1,6 = 14.36$, $P = 0.009$; Figure 5C).

EMG onset was significantly earlier in the supracoracoideus than in the pectoralis, measured with respect to the relevant wingbeat transition. During air density reduction trials, the supracoracoideus was activated 1 ms earlier (6.22 ± 1.22% earlier in the wingbeat), relative to the subsequent wingbeat transition, than the pectoralis ($F_{1,6} = 5.83$, $P = 0.044$; Figure 6A). During load lifting trials, the supracoracoideus was activated 1 ms earlier (4.18 ± 0.77 % earlier in the wingbeat), relative to the subsequent wingbeat transition, than the pectoralis ($F_{1,6} = 4.42$, $P = 0.035$; Figure 6C).

The EMG duration of the supracoracoideus was significantly longer in the supracoracoideus than in the pectoralis. On average, during air density reduction trials, the supracoracoideus was activated 0.80 ± 0.33 ms longer than the pectoralis ($F_{1,6}$ = 10.96, P = 0.016; Figure 6B). During load lifting trials, the supracoracoideus was activated, on average 0.72 ± 0.20 ms longer than the pectoralis ($F_{1,6}$ = 15.86, P = 0.007; Figure 6D).

Influence of air density on the relationship between muscle activation and wingbeat kinematics

Previous research in birds has demonstrated that normalized EMG area is a strongly correlated with peak muscle force, strain rate, and thus pectoralis power output during flight (Hedrick et al., 2003; Tobalske et al., 1997; Ellerby and Askew, 2007). Data presented here strongly suggest that as hovering power output requirements increase (with either decreasing air density or increasing load) flight muscle EMG area also increases. In order to understand whether air density influenced the translation of muscle activation into wingbeat kinematics we constructed a model which related EMG area, trial type, and the interaction of these two parameters, to the mean angular velocity of the wingtip. Individual was included as a random factor in the model design and models were fitted to the pectoralis and supracoracoideus separately. Using the languageR package (v. 1.4) in the R statistical programing environment we estimated confidence intervals and P-values for model parameters. As shown in Table 1, EMG area of the pectoralis or supracoracoideus were the only significant predictors of mean angular velocity of the wingtip in each model (pectoralis: P < 0.0001; supracoracoideus: P < 0.0001). Neither the experiment type, nor the interaction between experiment type and EMG area were significant predictors (P > 0.2 in all cases; see Table 1).

411

412 **Discussion**

413 Ruby-throated hummingbirds increased performance during sustained hovering (in air
414 density reduction and submaximal load lifting trials) primarily through increases in wing stroke
415 amplitude while increases in wingbeat frequency were only observed when hovering at the
416 lowest air density. Surprisingly, we did not observe significant increases in wingbeat frequency
417 during maximal load lifting assays. While data from the lowest air density trial appears to be
418 driving the trend in wingbeat frequency in our data, Chai and Dudley have previously reported a
419 consistent increase in wingbeat frequency in ruby-throated hummingbirds subjected to
420 progressive heliox replacement (Chai and Dudley, 1995; 1996). Thus, we feel confident that the
421 trend we observed reflects a biological relevant pattern. The differences in reliance on stroke
422 amplitude and/or wingbeat frequency increases to generate more power output dependent on the
423 nature of the flight challenge are consistent with findings from studies on a variety of small
424 hummingbird species (Wells, 1993; Chai and Dudley, 1995, 1996 Altshuler and Dudley 2003;
425 Altshuler et al., 2004; Altshuler and Dudley; 2010). However, this is the first study to report such
426 variation in kinematic adjustments and the first to investigate flight muscle EMG patterning in
427 individual hummingbirds subjected to asymptotic load lifting and multiple distinct challenges to
428 sustained hovering flight.

429 Ruby-throated hummingbirds activate each of the two major flight muscles with 1-3
430 simultaneous bursts of motoneuron action potentials, eliciting muscle fiber action potentials in
431 the pectoralis and supracoracoideus, prior to the corresponding wing stroke. The number of
432 spikes per EMG burst are similar to that seen in other hummingbirds, and are substantially lower
433 than observed in other avian taxa (Hagiwara et al., 1968; Altshuler et al., 2010; Tobalkse et al.,

2010; Hedrick et al., 2003; Ellerby & Askew, 2007; Tobalske & Dial, 1994). The increases in stroke amplitude observed during sustained hovering in hypodense air or while lifting submaximal loads was associated with increases in EMG burst intensity (area) but not changes in spike number per burst. The data presented here and in the previous studies just mentioned imply consistency in the neuromuscular and kinematic approaches to varying power output small hummingbirds employ during sustainable hovering or forward flight (Chai and Dudley, 1995; 1996; Wells, 1993; Altshuler et al., 2010; Tobalske et al., 2007; 2010). In contrast to sustained hovering, both EMG area and spike number per burst increased substantially in both the pectoralis and supracoracoideus in order to generate significantly greater stroke amplitudes and angular velocities during maximal load lifting, a pattern also seen in the pectoralis of Anna's hummingbirds (Altshuler et al., 2010). Overall, these data suggest that ruby-throated hummingbirds employ spatial recruitment of motor units to drive sustainable increases in stroke amplitude while both spatial and temporal recruitment of motor units is required to achieve the greatest stroke amplitudes at high wingbeat frequencies during burst hovering in both major flight muscles, a finding consistent with previous reports (Altshuler et al, 2010; Tobalske et al., 2010).

Steady hover-feeding in hypodense heliox gas mixtures and while lifting submaximal loads is an exclusively or predominantly aerobically-power activity given it can be sustained for more than several seconds and as evidenced by the simultaneous rise in estimated mechanical power output and oxygen consumption rate, and resulting invariant muscle efficiency (Chai and Dudley, 1996; Wells, 1993). In contrast, we assume asymptotic maximal load lifting is dependent on supplemental anaerobic metabolic power input because hummingbirds cannot sustain maximal hovering effort for more than approximately 1 sec and subsequently pant

heavily for a few moments after descending to the chamber floor. The distinctive EMG waveform patterns associated with differences in the sustainability of muscle performance are striking. Our data show that a given proportion of motor units are activated on average once per wingbeat in the pectoralis and once or twice per wingbeat in the supracoracoideus with each wingbeat at frequencies of approximately 55 – 60 Hz, and suggest that activation of fibers at this frequency is entirely aerobically powered. In contrast, the activation of a greater proportion of motor units, some potentially 2-3 times per wingbeat, during maximal hovering appears to surpass an aerobically sustainable threshold.

Evidence from sonomicrometry in the pectoralis in combination with high speed recordings and analysis of wingbeat kinematics suggests that the wings are "kinematically rigid" and that wingtip position is an accurate proxy of flight muscle strain (Tobalske et al., 2007). In ruby-throated hummingbirds, flight muscle activation begins about halfway into the prior half stroke, when each muscle is lengthening. In addition, we found EMG activity ceased in each flight muscle before the start of the subsequent half wingbeat, and thus, before muscle shortening, across all hovering behaviours examined, consistent with findings in Anna's and rufous hummingbirds (Altshuler et al., 2010; Tobalske et al., 2010). Because the wingbeat frequencies in each species were all greater than 40 Hz (Altshuler et al., 2010; Tobalske et al., 2010) it seems possible that the cessation of EMG activity prior to muscle shortening is a general feature of flight muscles operating near or above this frequency. Burst durations increased as mechanical power output requirements increased and were longest during maximal load lifting assays. Because burst duration was calculated as the time rectified EMG signal was different from 0 V, the significant increase in burst duration across sustained challenges while spike number remained constant is likely simply a reflection of the overall greater area (i.e. "height" ×

"width") of these individual EMG spikes. Importantly, the significant increase in burst duration and spike number seen during maximal load lifting mean the flight muscles maintain tension later into the wingbeat cycle. Since wingbeat frequency either stays the same or increases during maximal load lifting compared to sustained hovering in normodense air, this implies that the shorter EMG burst duration and synchrony of fiber activation observed during sustained hovering is not solely the consequence of a constrained activation window which would allow sufficient time for relaxation to occur. Rather, it is the maximal burst durations observed during brief load lifting which may be constrained within the maximum allowable activation window.

While stroke amplitude increased both as a function of lower air density and while birds sustainably lifted progressively more mass, wingbeat frequency also increased at low air densities. These findings confirm that interspecific variation in hovering flight behaviour does not, by itself, explain the differences in kinematics observed between flight challenge types previously (Wells, 1993; Chai and Dudley, 1995; 1996; Altshuler et al., 2010). Further analysis is required to determine if the differences in kinematics observed with each trial type are the result of active variation in neural programming, or the consequence of differences in drag imposed on the wing by variation in air density in one trial type, but not the other. Aerodynamic theory predicts that profile drag, which accounts for a significant portion of total calculated aerodynamic power requirements in hovering hummingbirds (Wells, 1993; Altshuler, 2001), decreases as air density declines. Thus, it is possible that for a given neuromuscular input, and resulting muscle force, lower profile drag may result in greater wing acceleration in hypodense air. We examined the effect of neural input on resulting wing acceleration by fitting a model with normalized EMG area, experiment type, and their interaction term as factors. Mean angular velocity of the wingtip was chosen as the dependent variable because this kinematic parameter

captures variation in both stroke amplitude and the duration of the wingbeat. Individual was included as a random factor. As shown in Table 1, only EMG area was found to be a significant predictor of variation in mean angular velocity of the wingtip. The fact that neither experiment type nor the interaction term were found to be significant predictors indicates that the relationship between neuromuscular input (i.e. relative intensity of muscle activation) and mean angular velocity is consistent regardless of air density. It is possible that other wingbeat parameters, such as attack angle, vary with air density in a way that offsets the decline in drag on the wing. However, assuming this is not the case, we hypothesize that while the wing may be accelerated more easily through hypodense air, achieving a comparatively greater mean angular velocity, each flight muscle must provide additional power to decelerate the wing in advance of the stroke transition.

We observed a slight trend towards increased wingbeat frequency during maximal load lifting compared to unweighted hovering in normdense air. However, in contrast to findings by Chai et al. (1997), this increase was not significant. Wingbeat frequencies of ruby-throated hummingbirds during hovering flight in normodense air were between 51- 57 Hz and frequencies during maximally loaded flight were between 54-58Hz. Chai et al. (1997) reported frequencies of 49 – 52 Hz for hovering flight in normodense air and frequencies of 57-58 Hz for maximally loaded ruby-throated hummingbirds. Although the range in the values between our two studies are comparable the wingbeat frequencies observed in our birds during unweighted hovering in normodense air were slightly higher than those in Chai et al. (1997). It is unclear if this discrepancy is due to anything more than sampling error or interindividual variation. However, it should be noted that the birds studied by Chai et al. (1997) were not implanted with electrodes. It is possible that implantation of the electrodes in our birds may have affected kinematic

performance. A study by Ellerby and Askew (2007) found that implanting both EMG electrodes and sonomicrometry transducers in zebra finches and budgerigars results in significant differences in wingbeat kinematics. Due to time constraints, it was not possible for us to obtain a full set of control data in birds prior to electrode implantation. Still, in contrast to our findings, Anna's hummingbirds that were instrumented with electrodes did increase wingbeat frequency during maximal load lifting assays (Altshuler et al., 2010). Anna's hummingbirds are about 1.5 times larger than ruby-throated hummingbirds and exhibit a lower and broader range of wingbeat frequencies than those observed in ruby-throated hummingbirds in our study or that by Chai et a. (1997). It is possible that electrode implantation also affected the wingbeat kinematics of hovering Anna's hummingbirds, though the effect was less pronounced. Unfortunately, data on the wingbeat kinematics of the individuals examined in the study by Altshuler et al. (2010) hovering while not implanted with electrodes is also unavailable.

In comparison to the pectoralis the supracoracoideus consistently exhibited more spikes per burst and burst duration was longer during all sustainable hovering trials. In addition, during all hovering behaviour, including maximal load lifting, the supracoracoideus was activated earlier prior to muscle shortening. The pectoralis and the supracoracoideus are both composed exclusively of type IIa (fast twitch oxidative-glycolytic) fibers (Suarez, 1992; Welch and Altshuler, 2009). Thus, significant differences in EMG waveforms between the two muscles cannot be related to variation in motor unit complement type or the relative activation timing of one motor unit type relative to another. We hypothesize two major differences in muscle anatomy may at least partly underlie the observed variation in EMG patterning. First, while the homogenous complement of fibers in each muscle produce similar force per unit fiber cross-sectional area (Reiser et al. 2013) the physiological cross-sectional area of the supracoracoideus

is substantially smaller. Thus, if a similar proportion of fibers are activated in each muscle, the supracoracoideus will produce less overall power output than the pectoralis. Because the hovering wingbeat is relatively symmetrical, it is possible that the power output requirements from each muscle are, unlike their sizes, also relatively similar. As shown in this study and elsewhere (Altshuler et al., 2010; Tobalske et al., 2010), increases in temporal recruitment of fibers within a given hummingbird flight muscle, reflected as increases in spike number per burst, correlate with increased power output. Therefore, it seems plausible that the longer EMG duration and greater spike number per burst in the supracoracoideus compared to the pectoralis reflects relatively greater temporal recruitment of motor units in response to greater power demands per unit muscle mass. The second anatomical difference may underlie the earlier activation, relative to muscle shortening, observed in the supracoracoideus. The muscle-tendon unit anatomy is distinctly different between the pectoralis and supracoracoideus. Though the supracoracoideus originates on the keel of the sternum, deep to the pectoralis, the distal tendon passes through the shoulder and inserts on the dorsal side of the humerus acting to elevate the wing (Zusi and Bentz, 1984). No long tendon attaches to the pectoralis at either its origin or insertion points. We hypothesize that neural activation occurs earlier in the supracoracoideus relative to muscle-tendon unit shortening because there is greater compliance of series elastic components (principally, this long tendon). Generally, the long, thin tendons attached to the belly of pennate distal hindlimb muscles of vertebrates with short fibres, are highly compliant (Roberts, 2002). Muscles with tendons that are highly compliant expend a large fraction of their shortening capacity stretching the tendon rather than causing skeletal movements directly. If, as we hypothesize, there is greater elastic compliance in the wing elevator muscle (supracoracoideus) than in the depressor (pectoralis) of hummingbirds, then it follows that the

572 contribution of elastic energy storage and recovery may play a relatively greater role in the
573 deceleration and subsequent reacceleration of the wing during the downstroke-to-upstroke
574 transition. Such asymmetry of elastic energy recovery in the otherwise relatively symmetrical
575 hummingbird hovering wingbeat should be considered as the finer aspects of cumulative power
576 output during hovering are investigated.

577 The neuromuscular encoding of modulation of wingbeat kinematics during sustained
578 hovering flight appears highly conserved across species and hovering flight challenges. Ruby-
579 throated hummingbirds adopt subtly different kinematic solutions to adjust flight performance
580 when lifting sustainable loads as opposed to when hovering in hypodense air. Despite the
581 reduction in drag on the wing, high stroke amplitudes at moderately higher wingbeat frequencies
582 while hovering in hypodense air necessitate comparable increases in flight muscle activation,
583 presumably as higher forces are needed to decelerate the wings prior to stroke transition. The
584 high wingbeat frequencies of ruby-throated hummingbirds limit the amount of time available for
585 the activation and deactivation of primary flight muscles. The limited activation window has
586 resulted in motor unit recruitment being highly synchronized. With a single fiber type present in
587 both major flight muscles, and one or two spike per burst during all sustained flight behaviours,
588 it seems Anna's (Altshuler et al., 2010), rufous (Tobalske et al., 2010), and ruby-throated
589 hummingbirds (this study) all modulate power output at high operating frequencies largely or
590 exclusively by varying spatial recruitment in each muscle. Nonetheless, the fact that
591 hummingbirds can increase spike number and burst duration during maximal burst hovering
592 suggests that constraints on burst duration during sustained hovering are aerobic, rather than
593 mechanical. While these results confirm that the relatively symmetrical hummingbird wingbeat
594 is achieved by relatively similar changes in the intensity of activation of the antagonist primary

flight muscles, variation in the timing of activation and number of spikes per EMG burst were consistently different between the two muscles, likely reflecting differences in muscle morphology and compliance.

Acknowledgements

Shanchai Zahid, Derrick Groom, and Piravinthan Sithamparanathan assisted in collection of the data. We thank Douglas Altshuler for providing custom-authored MATLAB analysis tools, for guidance regarding data analysis, and for helpful discussion. We thank Mahinda Samarakoon for assistance with coding in R. We also thank two anonymous reviewers for their comments. Funding for this research was provided by a Natural Sciences and Engineering Research Council of Canada (NSERC) Discovery Grant (#386466), a Canada Foundation for Innovation (CFI) Leaders Opportunity Fund grant (#25326), and an Ontario Research Fund, Research Infrastructure grant (#25326) to KCW.

References

Altshuler, D. L. (2001). Ecophysiology of Hummingbird Flight Along Elevational Gradients: An Integrated Approach.

Altshuler, D. L. and Dudley, R. (2003). Kinematics of hovering hummingbird flight along simulated and natural elevation gradients. *J. Exp. Biol.* **206**, 3139-3147.

Althsuler, D. L., Dudley, R., Heredia, S.M. and McGuire, J. A. (2010). Allometry of hummingbird lifting performance. *J. Exp. Bio.* **213**, 725-734.

Althsuler, D. L., Dudley, R. and McGuire, J. A. (2004). Resolution of a paradox: Hummingbird flight at high elevation does not come without a cost. *Proc. Natl. Acad. Sci.* **101**, 17731-17736.

Althsuler, D. L, Quicazán-Rubio, E. M., Segre, P. S. and Middleton, K. M. (2012). Wingbeat kinematics and motor control of yaw turns in Anna's hummingbirds *(Calypte anna). J. Exp. Biol. **215**, 4070-4084.*

Altshuler, D. L, Welch, K. C, Cho, B. H., Welch, D.B, Lin, A. F., Dickson, W. B. and Dickinson, M. H. (2010). Neuromuscular control of wingbeat kinematics in Anna's hummingbirds (*Calypte anna*). *J. Exp. Biol.* **213**, 2507-2514.

Askew, G. N. and Marsh, R. L. (1998). Optimal shortening velocity (V/Vmax) of skeletal muscle during cyclical contractions: length-force effects and velocity dependent activation and deactivation. *J. Exp. Biol.* **201**, 1527-1540.

Askew, G. N. and Marsh, R. L. (1997). The effects of length trajectory on the mechanical power output of mouse skeletal muscles. *J. Exp. Biol.* **200**, 3119-3131.

Chai, P., Chen, J. S. C. and Dudley, R. (1997). Transient hovering performance of hummingbirds under conditions of maximal loading. *J. Exp. Biol.* **200**, 921-929.

Chai, P. and Dudley, R. (1995). Limits to vertebrate locomotor energetic suggested by hummingbirds hovering in heliox. *Nature.* **377**, 722-725.

Chai, P. and Dudley, R. (1996). Limits to flight energetics of hummingbirds hovering in hypodense and hypoxic gas mixtures. *J. Exp. Biol.* **199**, 2285-2295.

Chai, P. and Dudley, R. (1999). Maximum flight performance of hummingbirds: capacities, constraints, and trade-offs. *Am. Nat.* **153**, 398-411.

Degernes, A. L. and Feduccia, A. (2001). Tenectomy of the supracoracoideus muscle to deflight pigeons (*Columba livia*) and cockatiels (*Nymphicus hollandicus*). *J. Avian Med. Surg.* **15**, 10-16.

Ellerby, D. J. and Askew, G. N. (2007). Modulation of pectoralis muscle function in budgerigars *Melopsitaccus undulatus* and zebra finches *Taeniopygia guttata* in response to changing flight speed. *J. Exp. Biol.* **210**, 3789-3797.

Greenewalt, C. H. (1962). Dimensional relationships for flying animals. *Smithsonian Misc. Collections.* **144**, 1- 46.

Hagiwara, S., Chichibu, S. and Simpson, N. (1968). Neuromuscular mechanisms of wing beat in hummingbirds. *Z. Vergl. Physiol.* **60**, 209-218.

Hedrick, T. L., Tobalske, B. W. and Biewner, A. A. (2003). How cockatiels modulate pectoralis power output across flight speeds. *J. Exp. Biol.* **206**, 1363-1378.

Reiser, P. J., Welch Jr., K. C., Suarez, R. K., and Altshuler, D. L. (2013) Very low force-generating ability and unusually high temperature dependency in hummingbird flight muscle fibers. *J. Exp. Biol.* **216**, 2247-2256.

Roberts, T. J. (2002). The integrated function of muscles and tendons during locomotion. *Comp. Biochem. and Physiol A.* **133**, 1087-1099.

Sokoloff, A. J., Gray-Chickering, J., Harry, J. D., Poore, S. O. and Goslow, G. E., Jr (2001). The function of the supracoracoideus muscle during takeoff in the European starling (*Sternus vulgaris*): Maxheinz Sy revisited. In *New Prespectives on the Origin and Early Evolution of Birds: Proceedings of the International Symposium in Honor of John H. Ostrom* (ed. J. Gauthier and L. F. Gall), pp. 319-332. New Haven: Peabody Museum of Natural History.

Suarez, R.K. (1992). Hummingbird flight: sustaining the highest mass-specific metabolic rates among vertebrates. *Experientia.* **48**, 565-569.

Tobalkse, W. (2007). Biomechanics of bird flight. *J. Exp. Biol.* 2010, 3135-3146.

Tobalkse, W. (2010). Hovering and intermittent flight in birds. *Bioinspir. Biomim.* **5**, 1-10.

Tobalske, B. W. and Biewener, A. A. (2008). Contractile properties of the pigeon supracoracoideus during different modes of flight. *J. Exp. Biol.* **211**, 170-179.

Tobalkse, B. W., Biewener, A. A, Warrick, D. R., Hedrick, T. L. and Powers, D. R. (2010). Effects of flight speed upon muscle activity in hummingbirds. *J. Exp. Biol.* **213**, 2515-2523.

Tobalske, B. W. and Dial, K. P. (1994). Neuromuscular control and kinematics of intermittent flight in budgerigars *(Melopsittacus undulatus). J. Exp. Biol.* **187**, 1-18.

Tobalkse, B. W., Hedrick, T. L., Dial, K. P. and Biewener, A A. (2003). Comparative Power Curves in bird flight. *Nature*, **421**, 363-366.

Tobalkse, B. W., Olson, N. E. and Dial, K. P. (1997). Flight style of black-billed magpie: variation in wing kinematics, neuromuscular control, and muscle composition. *J. Exp. Zool.* **279**, 313-329.

Tobalske, B. W., Warrick, D. R, Clark, C. J., Powers, D. R., Hedrick, T. L., Hyder, G. A. and Biewener, A. (2007). Three-dimensional kinematics of hummingbird flight. *J. Exp. Biol.* **210**, 2368-2382.

Warrick, D. R., Tobalske, B.W. and Powers, D. R. (2005). Aerodynamics of the hovering hummingbird. *Nature*. **453**, 1094-1097.

Warrick, D. R., Tobalske, B. W. and Powers, D. R. (2009). Lift Production in the Hovering Hummingbird. *Proc. R. Soc. B.* **276**, 3747-3752.

Welch, K. C. and Altshuler, D. L. (2009). Fiber type homogeneity of the flight musculature in small birds. *Comp. Biochem. Physiol. B* **152**, 324-331.

Wells, D. J. (1993). Ecological correlates of hovering flight of hummingbirds. *J. Exp. Biol.* **179**, 59-70.

Zusi, R., Bentz, D. (1984) Myology of purple-throated carib (*Eulampis jugularis*) and other hummingbirds (Aves: Trochilidae). *Smithson. Contrib. Zool.* **385**, 1-70.

Table 1. Mixed effects regression model of the relationship between mean angular velocity of the wingtip during hovering, the intensity of muscle activation (normalized EMG area), and the experiment type (air density reduction or load lifting). Note: individual is included as a random effect.

Figure 1. Experimental set-up for *in vivo* recordings under multiple hovering challenges. A) Air density reduction trials and unweighted hovering in normodense air were examined while a hummingbird fed from a suspended feeder. A high-speed video camera recorded wingbeat kinematics from an overhead view. Biploar electrodes were inserted into the left pectoralis and supracoracoideus of the bird. During hypodense condition, air density was decreased by progressive replacement of ambient in the airtight chamber with heliox. Unweighted hovering trials were conducted using an identical setup except that no heliox replacement was attempted. B) Sub-maximal load lifting trials were performed as each bird hover fed in normodense air while lifting 0.25, 0.5, or 0.75 g strings of beads placed around its neck. 3) Maximal load lifting performance in normodense air was assessed as each bird was placed at the bottom of the arena with a string of color-coded beads was fixed around its neck via a harness. The birds flew upwards until the weight of the beads lifted off the floor equalled the maximum they could briefly bear while transiently hovering.

Figure 2. An illustration of the musculoskeletal anatomy of small hummingbirds (modified from Welch and Altshuler, 2009). Markings indicate the position of electrode placement in (A) the pectoralis and (B) the supracoracoideus muscle. Note the illustration in B is identical to that in A except that the pectoralis has been removed to show the supracoracoideus muscle, which lies deep to it.

Figure 3. Wingbeat kinematics [stroke amplitude (A, C) and wingbeat frequency (B, D)] in relation to experimental treatments [air density (A, B) or total mass lifted (C, D)] for hovering ruby-throated hummingbirds (*Archilochus colubris*). Data are binned according to treatment level. Symbols represent mean (± s.d.) of N = 4 individuals. Trend lines are for illustration only and added only when variation in the data across treatment means was significant.

Figure 4. Sample EMG recordings of both flight muscles while the bird was hovering in ambient air lifting 0.75 g in excess of body mass. Using detection criteria defined in the methods section exactly 1 spike per burst in the pectoralis and 2 spikes per burst in the supracoracoideus were counted in each of the bursts shown. Note: signals are direct outputs from the amplifier with

analog filter cut-offs of 1 Hz and 10 kHz, prior to any post processing. Shaded areas correspond to the downstroke of the wing.

760 Figure 5. Number of spikes per (A, C), and normalized EMG area of (B, D), electromyogram
761 bursts in the pectoralis and supracoracoideus of in relation to experimental treatments [air
762 density (A, B) or total mass lifted (C, D)] for hovering ruby-throated hummingbirds (*Archilochus*
763 *colubris*). Data are binned according to treatment level. Values for the pectoralis and
764 supracoracoideus are offset slightly for clarity. EMG area is normalized within individuals to the
765 maximum value recorded across all trials. A threshold value of 0.25 of the maximum spike
766 intensity within an individual trial (hovering at a given air density or with a given mass lifted)
767 was applied to automate the detection of individual spikes within bursts. Symbols represent mean
768 (± s.d.) of N = 4 individuals.

769

770 Figure 6. Timing (onset of EMG activity prior to ensuing wingtip reversal; A, C) and duration of
771 the EMG burst (B, D) in the pectoralis and supracoracoideus of in relation to experimental
772 treatments [air density (A, B) or total mass lifted (C, D)] for hovering ruby-throated
773 hummingbirds (*Archilochus colubris*). Data are binned according to treatment level. Values for
774 the pectoralis and supracoracoideus are offset slightly for clarity. Symbols represent mean (±
775 s.d.) of N = 4 individuals.

776

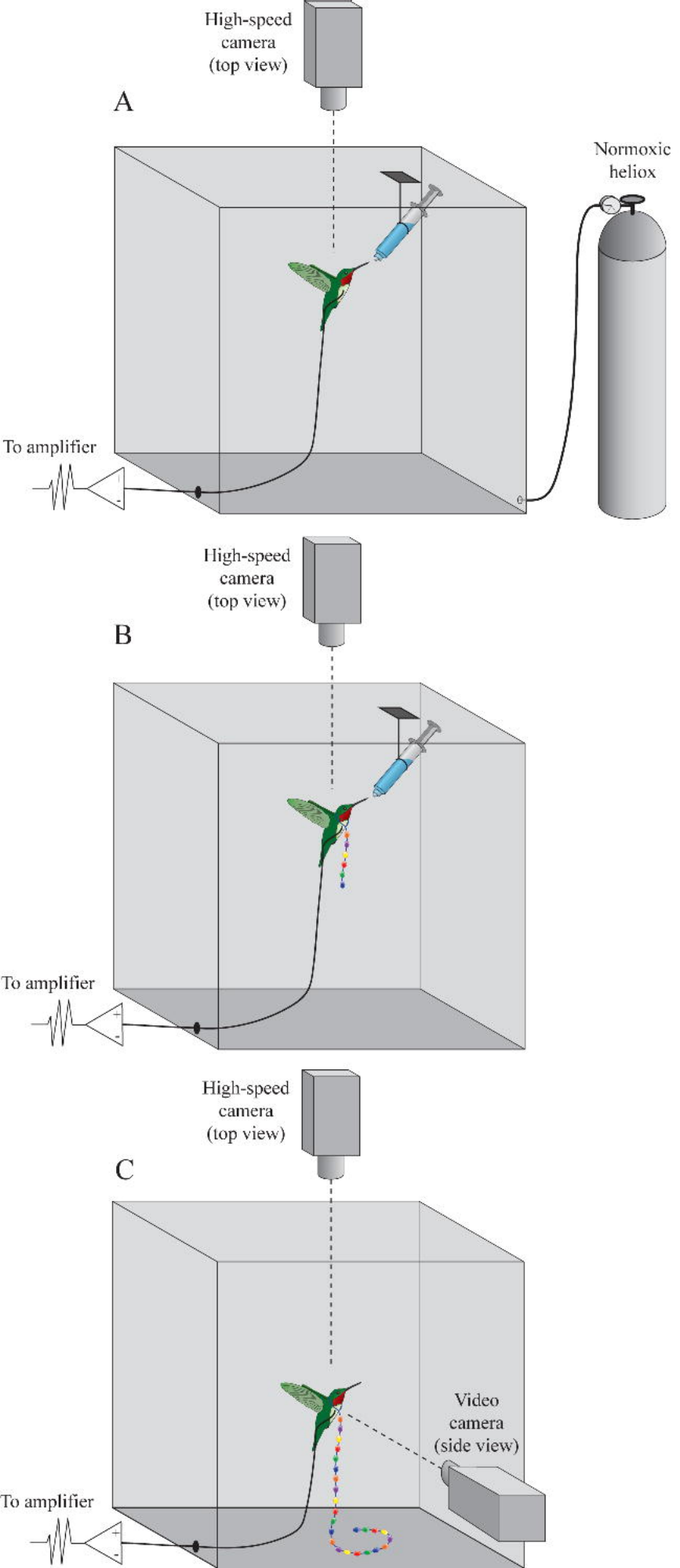
High-speed
camera
(top view)
A
Normoxic
heliox
To amplifier
High-speed
camera
(top view)
B
To amplifier
High-speed
camera
(top view)
C
Video
camera
(side view)
To amplifier

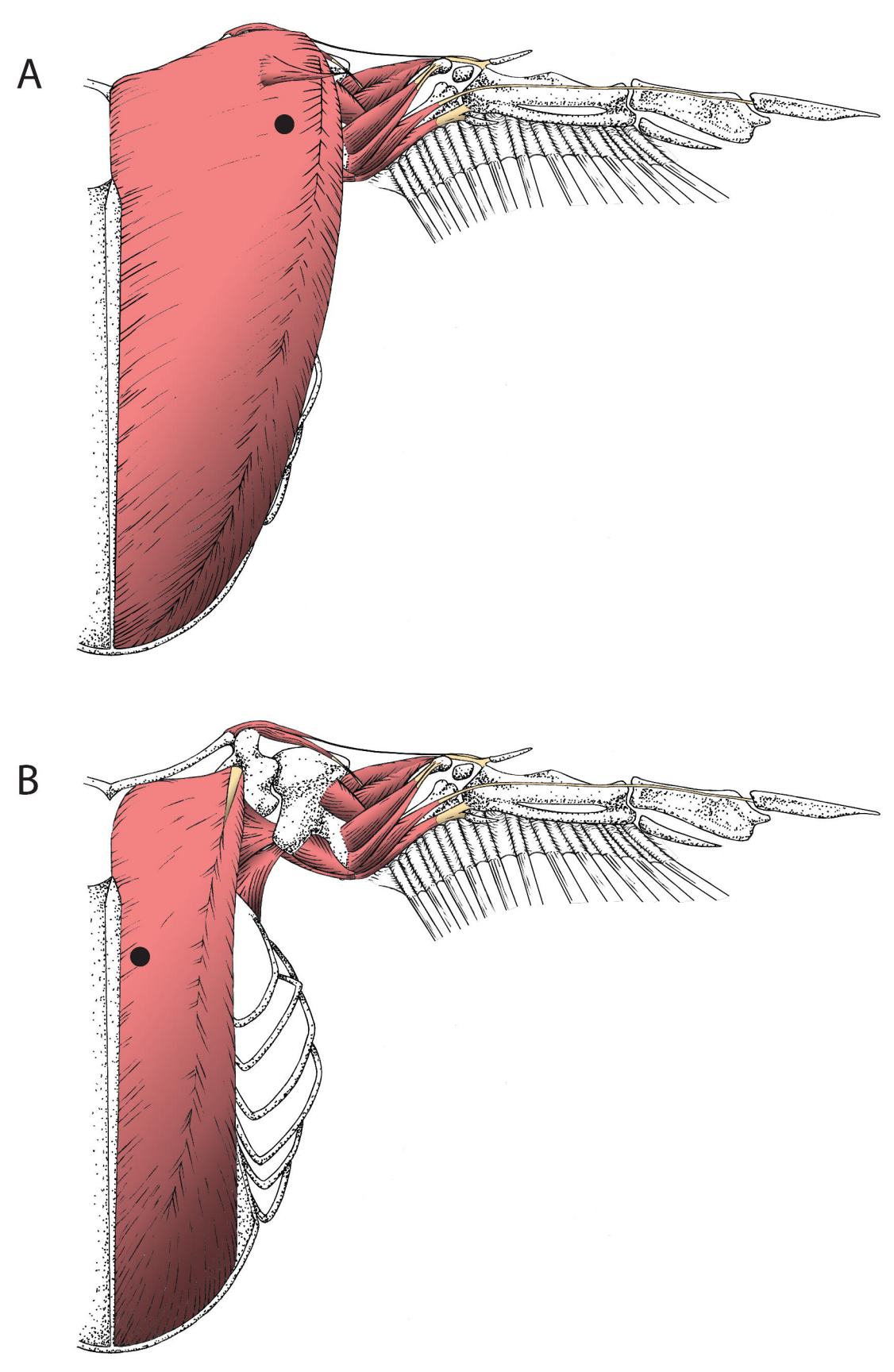
A
B

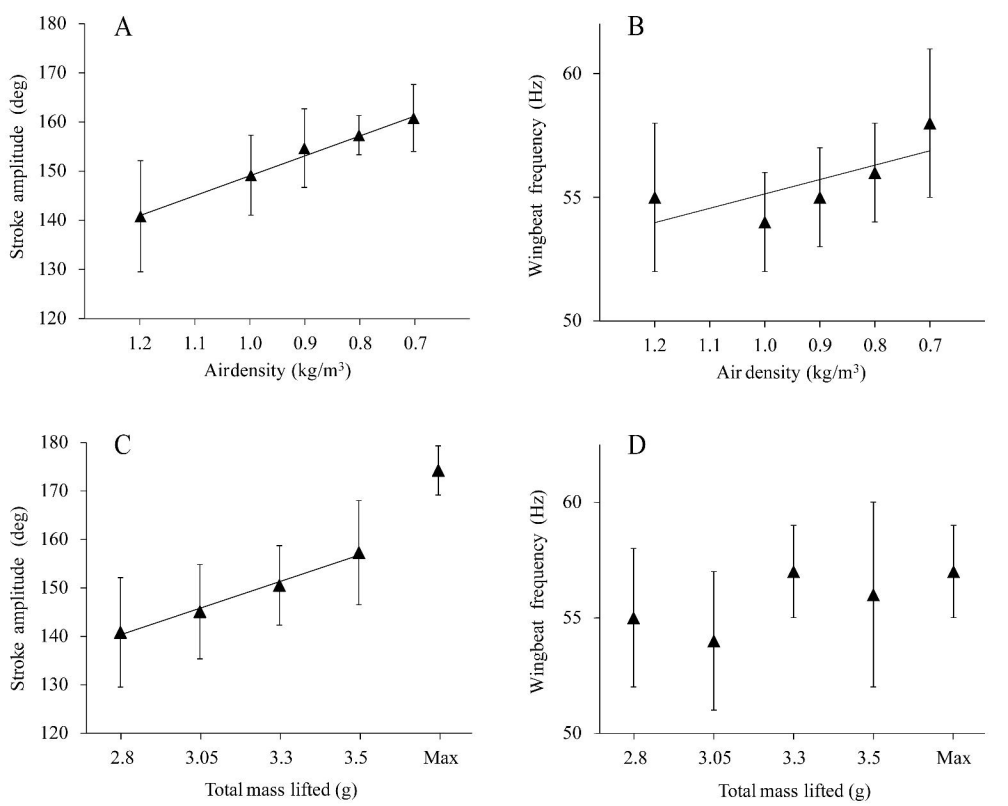
A
Stroke amplitude (deg)
180
170
160
150
140
130
120
1.2
1.1
1.0
0.9
0.8
0.7
Airdensity (kg/m3)
B
Wingbeat frequency (Hz)
60
55
50
1.2
1.1
1.0
0.9
0.8
0.7
Air density (kg/m3)
C
Stroke amplitude (deg)
180
170
160
150
140
130
120
2.8
3.05
3.3
3.5
Max
Total mass lifted (g)
D
Wingbeat frequency (Hz)
60
55
50
2.8
3.05
3.3
3.5
Max
Total mass lifted (g)

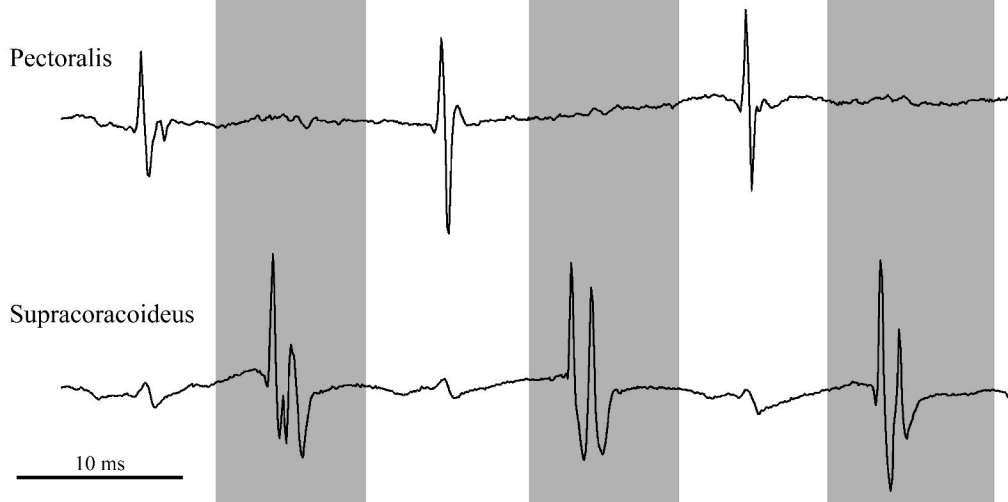
Pectoralis
Supracoracoideus
10 ms

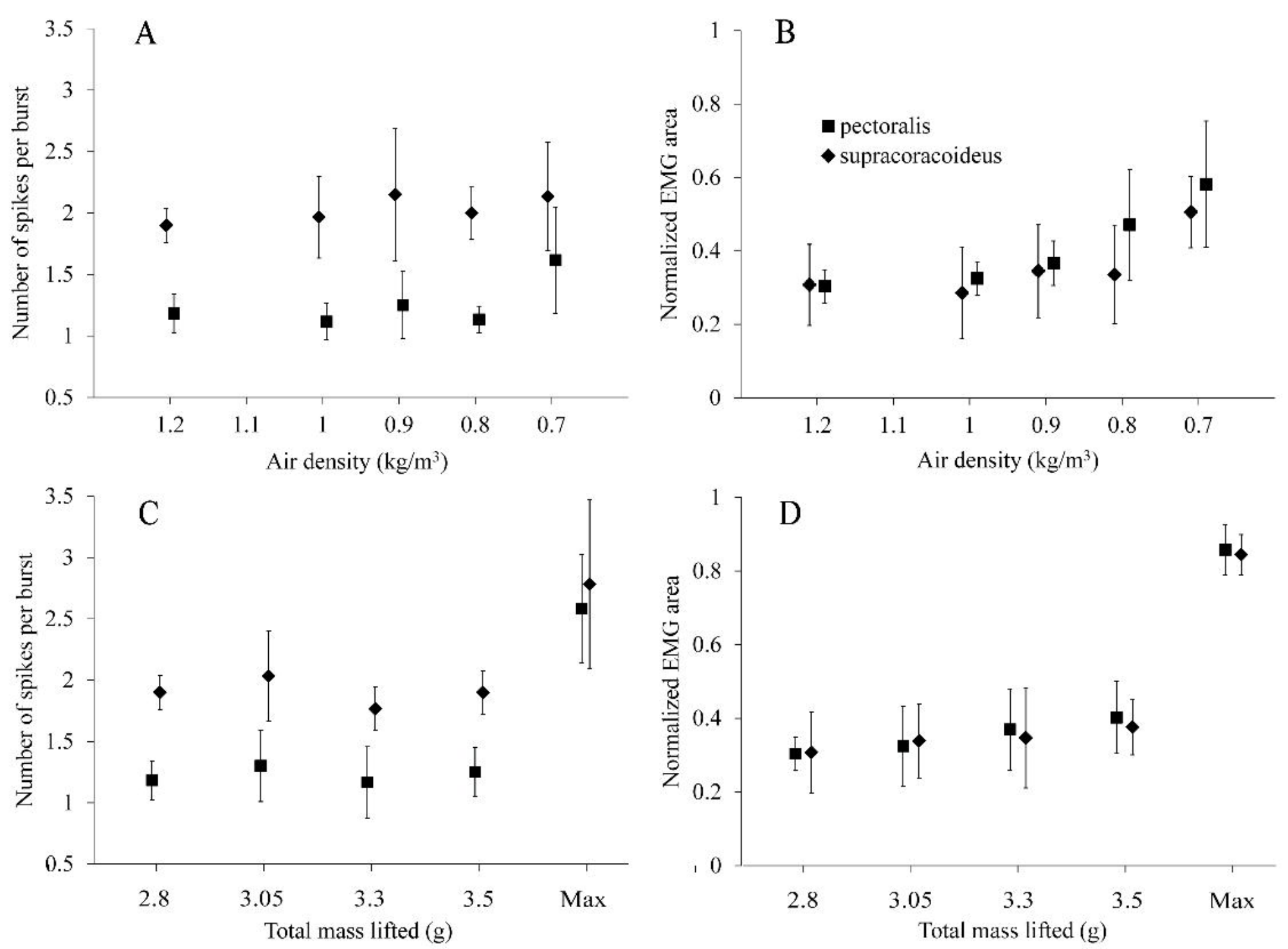
A
Number of spikes per burst
3.5
3
2.5
2
1.5
1
0.5
1.2
1.1
1
0.9
0.8
0.7
Air density (kg/m3)
B
Normalized EMG area
1
0.8
0.6
0.4
0.2
0
pectoralis
supracoracoideus
1.2
1.1
1
0.9
0.8
0.7
Air density (kg/m3)
C
Number of spikes per burst
3.5
3
2.5
2
1.5
1
0.5
2.8
3.05
3.3
3.5
Max
Total mass lifted (g)
D
Normalized EMG area
1
0.8
0.6
0.4
0.2
0
2.8
3.05
3.3
3.5
Max
Total mass lifted (g)

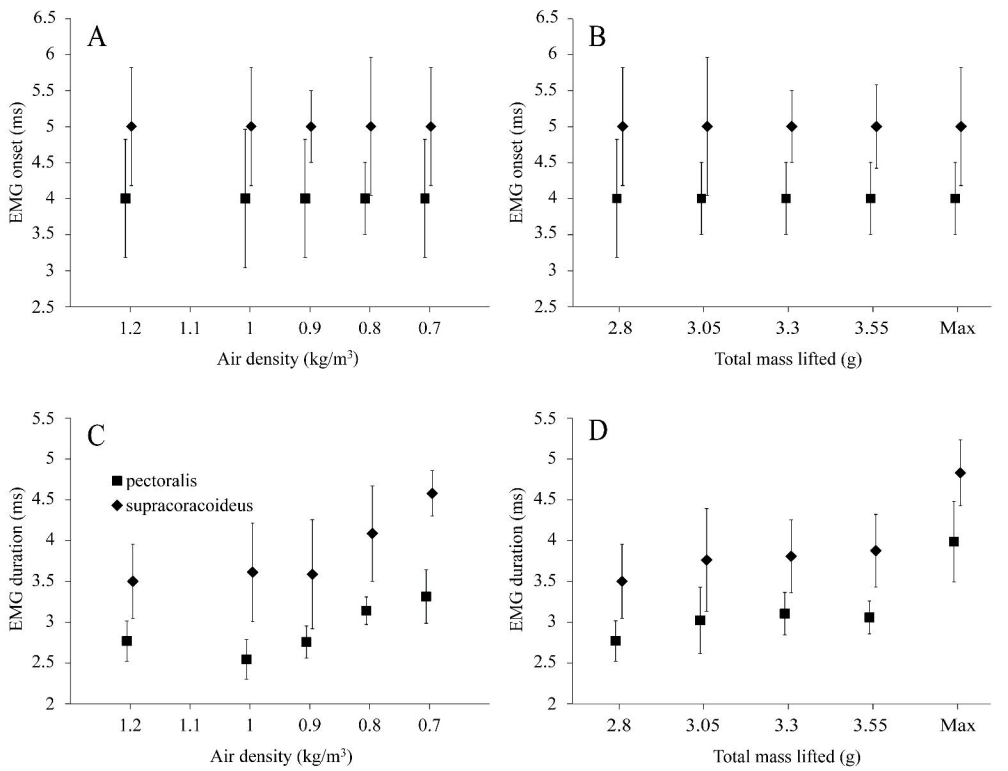
A
B
C
D
EMG onset (ms)
EMG duration (ms)
6.5
6
5.5
5
4.5
4
3.5
3
2.5
2
1.2
1.1
1
0.9
0.8
0.7
Air density (kg/m3)
2.8
3.05
3.3
3.55
Max
Total mass lifted (g)
pectoralis
supracoracoideus

		Mean angular velocity of the wingtip	
Muscle	Parameter	95% CI Estimate	*P* value
Pectoralis	EMG area	(60.58, 117.04)	< 0.0001*
	Experiment type	(-26.34, 61.05)	0.4133
	EMG area × Experiment Type	(-184.29, 47.21)	0.2358
Supracoracoideus	EMG area	(59.97, 216.39)	< 0.0001*
	Experiment type	(-34.36, 46.86)	0.9231
	EMG area × Experiment Type	(-167.14, 59.70)	0.4471